

Thickness and crustal composition investigation in the Sul-rio-grandense Shield (SrgS), Southern Brazil

Ingrid Herzog^{*1**2}, Diogo Luiz de Oliveira Coelho², Nicolas Rodrigues Hispagnol², Marcus Vinicius Aparecido Gomes de Lima¹, Tiago Rafael Gregory¹, ¹Universidade Federal do Pampa (UNIPAMPA), ²Observatório Nacional (ON-RJ)

Copyright 2023, SBGf - Sociedade Brasileira de Geofísica

This paper was prepared for presentation during the 18th International Congress of the Brazilian Geophysical Society held in Rio de Janeiro, Brazil, 16-19 October 2023.

Contents of this paper were reviewed by the Technical Committee of the 18th International Congress of the Brazilian Geophysical Society and do not necessarily represent any position of the SBGf, its officers or members. Electronic reproduction or storage of any part of this paper for commercial purposes without the written consent of the Brazilian Geophysical Society is prohibited.

Abstract

The work aimed to study the discontinuities present in the layers inside the Earth, and their contributions to the understanding of the local geodynamics. In this context, the depth of the Mohorovicic Discontinuity and the crustal composition of the Sul-rio-grandense Shield (SrgS) was performed using the Receiver Function method and the *H-k stacking* program, respectively. For this preliminary work, seismic event data was gathered from two seismographic stations: CPSB and PLTB. The reference depth value for the Moho depth (37 km) was used as an input parameter to perform 3D inversion of the gravimetric data. This value was based on the results obtained from the *H-k stacking* method, which yielded values of 37.97 km for CPSB and 37.7 km for PLTB. The results of this study indicate a mafic and thin crust in comparison with other regions in the southern part of Brazil. The methods showed a good correlation in the values found, and proved to be efficient and promising in studying the undulation of the Moho in the SrgS.

1. Introduction

There are two models for dividing the Earth into distinct layers: one based on chemical composition and other based on the rheology of the materials (physical properties). The layers that constitute the Earth's interior, there exist various discontinuities, such as the Mohorovicic, Gutenberg, and Lehmann discontinuities (Press et al., 2006), which represent changes in composition or physical properties. Understanding the Earth's internal structure is crucial for geodynamic studies and the study of natural phenomena, such as seismic events (Kawakatsu et al., 2009; Kumar and Kawakatsu, 2011; Fischer and Rychert, 2010).

The depth of the Moho, which is a seismic discontinuity between the crust and the mantle, ranging from 30 km to 70 km on continents and from 7 km to 8 km in oceans (Fowler, 1990; Stein and Wysession, 2003). It is a crucial marker for understanding the geodynamic processes that have occurred in the region.

In the tectonic context, the study area comprises the geomorphological province of the Sul-rio-grandense Shield. For calculating the Moho depth, indirect methods of solid Earth geophysics were used, specifically seismological and gravimetric methods. In seismology, two seismographic stations were used, located very close to the edge of the SrgS (Fig. 1), which are associated with the Caçapava do Sul and Porto Alegre suture zones (Fernandes et al., 1995) (Fig. 2).

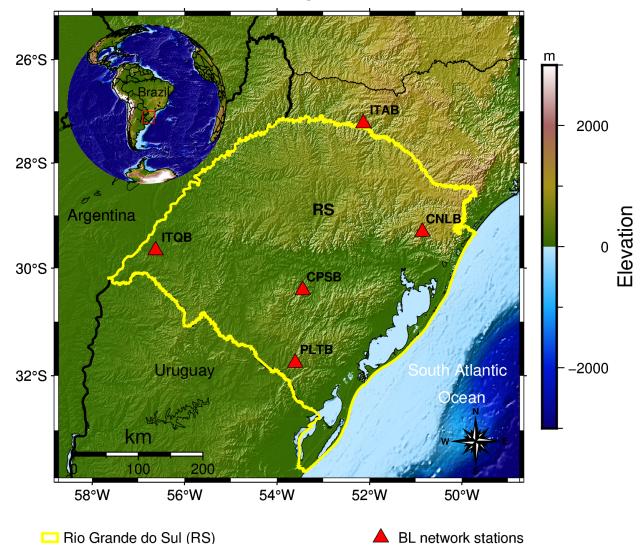


Figure 1 - Topo-altimetric location map (TOPODATA - Brazil, 2008) with location of the permanent seismic stations (red triangles) and with the SrgS region outline (white polygon).

The Receiver Function (RF) method is based on the times between the arrival of the primary wave and its respective refractions and reflections at seismic discontinuities in the vicinity of the seismographic station. Subsequent linear stacking analysis of these records generates information about the crustal composition and depth/thickness of the Moho beneath the station.

The information acquired by seismology provided input parameters for performing a 3D gravimetric inversion in the SrgS region to estimate the depth of the Moho based on data extracted from the World Gravity Map 2012 (WGM2012) compilation (Bonvalot, 2012). The aim of this study is to estimate the variation in depth and crustal composition of the Sul-rio-grandense Shield (SrgS) (Fig. 1). The findings of this work indicate a relatively thin mafic crust in comparison to other regions in the southern

part of Brazil, particularly in the stations located under the northern region of the Paraná Basin, which corroborates with the location of the Rio Grande Arch, which is characterized by flexures at the lithosphere level and by the uplift of the basement (horst). Being this event, possibly responsible for raising Moho leaving her more superficial. Therefore, this study corroborates the understanding of how the formation dynamics of the southern region of Brazil was.

2. Tectonic context

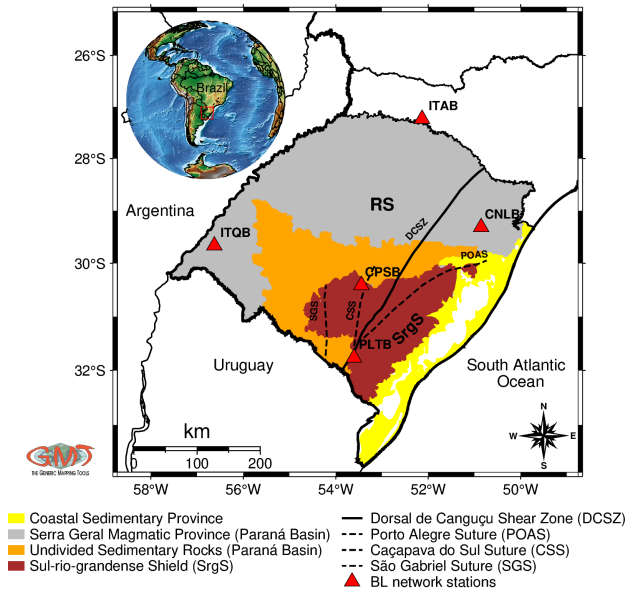


Figure 2 - Map of the geological context of the study area. Modified from Viero and Silva (2010).

2.1. Sul Rio-grandense Shield

The SrgS is composed of metamorphic, igneous, and sedimentary rocks, related to the pre-, syn-, and post-collisional stages of the Brasiliano orogeny in the Neoproterozoic (Hartmann et al., 2007). The formation of the majority SrgS units is interpreted as a continuation of the pre-Brasiliano Rio de la Plata Craton in Rio Grande do Sul (Fragoso César, 1980; Fragoso César et al., 1987; Basei, 1985), representing mainly an orogenic belt established on its margin during the Neoproterozoic. However, late intrusive bodies have an important contribution to the structural framework of the region (Ribeiro, 1970; Nardi & Bitencourt, 1989; Remus, 1999). The seismographic stations of the present study are located within the Brasiliano age deformation belt.

2.2. Paraná Basin

The Paraná Basin is composed of sedimentary layers, with a depocenter that has a cumulative thickness of about 7.5 km, of which 5.5 km are sediments deposited over a period of 385 million years, starting in the Ordovician and ending in the Cretaceous (Milani, 1997). The Paraná Basin has the largest fissural volcanism observed in the continental region, which resulted in the accumulation of 2 km of basalts over its sediments (Milani & Thomaz Filho, 2000).

3. Methodology

3.1 Seismology

In seismology, there are different techniques used to estimate the crustal thickness and composition beneath seismographic stations. In this study, we utilized the P-wave Receiver Function method (Langston, 1979) via the *SeisPy* package (Xu & He, 2022) and the *H-k stacking* program (Zhu & Kanamori, 2000) for subsequent linear stacking and analysis of these results. The database was created and processed using the *ObsPy* package (Krischer et al., 2015).

3.1.1. Data base (*ObsPy*)

The Brazilian Seismographic Network (RSBR) database was utilized in this study, the CPSB and PLTB stations were selected for analysis are respectively situated in the southern region of Rio Grande do Sul, specifically in Pelotas/Pedras Altas and Caçapava do Sul. These stations are located over the SrgS, near the boundary with the Paraná Basin. The stations used consist of a broadband seismometer and a built-in digitizer, which digitizes the seismograms at a rate of 100 samples per second.

For the catalog, events with magnitudes greater than 5.5 Mb and epicentral distances between 30 and 90° (Rivadeneira-Vera et al., 2019) occurred during the period from 2013 to March 2023. The epicentral distances in question are employed for the purpose of avoiding the phenomenon of triplication, which occurs between 15° and 30°, due to abrupt increases in velocities recorded in the upper mantle and the maximum epicentral distance to avoid shadow zones, which occur above 100° (Dourado, J.C. et al., 2007). Additionally, by adhering to such conditions, it is possible for the P-waves to impinge beneath a station with an orientation close to vertical, resulting in significantly larger amplitudes in the vertical component of the seismometer. On the other hand, the Ps waves (converted) during the refraction process in sub-horizontal discontinuities will exhibit more pronounced amplitudes in the horizontal components. With the established minimum magnitude, we ensure that the signal-to-noise ratio is higher, which allows for less error in the determination of the converted wave (Ps).

The P-wave Receiver Function method (Langston, 1979) was applied to obtain estimates of crustal thickness and composition. The *IASP91* velocity model was used to estimate the travel time of the P-wave (Kennett 1991), which was used to request seismograms of each event. Each seismogram was then filtered using a band-pass filter with cutoff frequencies of 0.05 and 2 Hz and a Hamming function was also applied to smooth out the edge effects of the signal, which reduces the spectrum interference (Hamming, R. W., 1974). The waveforms were saved in SAC (Seismic Analysis Code) format (Goldstein et al., 2005).

3.1.2. Receiver Function Method (*SeisPy*)

Rocks and structures play a crucial role in modifying the features of elastic waves that propagate from source to receiver. As a result of this, the seismogram recorded at a station is substantially affected by a number of factors (convolution of different signatures and responses). Among these factors, the type of pulse generated by the

Herzog, I; Coelho, D. L. O; Hispagnol, N. R; Lima, M. V. A. G; Gregory, T. R

seismic source, the intrinsic response of the recording instruments, including the type of seismometer and recorder used, as well as the influence of the complex signature of the medium through which the waves propagated, stand out.

The fundamental idea of the method involves the propagation of P waves generated by teleseismic events, which, upon incident on an interface separating two different media compositions, tend to undergo an abrupt change in speed due to the pronounced difference in physical properties, such as density. In this process, a small part of the incident P waves are converted into S waves (Ps), these converted phases arrive at the station after the main P phase. The seismogram also records the reflected multiples (PpPs and PpSs + PsPs), which are generated by the reverberations in the crust and travel greater distances than other seismic phases. Due to the previously mentioned factor, these waves are subject to greater variations and interference from the conversion of P to S in intracrustal discontinuities, for this same reason, it becomes difficult to identify these phases (Richter, 2014). (Richter, 2014).

Based on the time difference between the arrivals of P and Ps waves at the station (depending on the depth and speed contrast) and the amplitude of the waves (depending on the density and speed contrast) we obtain information about the structure of the planet's interior. Receiver Function (RF) is constructed by removing source, the instrumental response and deep mantle propagation effects (Richter, 2014). First, the S wave field is separated from the P wave field by a rotation from the station coordinate system (ZNE - vertical, north, east) to the ZRT wave coordinate system (vertical, radial, transverse), based on the back-azimuth (the value of the angle ($^{\circ}$) in relation to the geographic north, between the station and the epicenter of the event). This rotation is based on the polarization direction of the P and S waves, where the radial component (positioned parallel to the wave propagation direction) is perpendicular to the S wave propagation direction and the P wave will be perpendicular with the transverse component registering the S wave better.

Subsequently, the vertical component waveform is decomposed from the other components, the radial and transverse, thus removing the previously mentioned effects and the waveforms resulting from the Receiver Function are the Radial and Transverse components of each event (Richter, 2014).

Along with the deconvolution of the events, as explained above (the method used was the iterative deconvolution which is performed in the time domain (Kikuchi and Kanamori, 1982; Ligorria and Ammon, 1999), another filtering step (low-pass) was necessary to remove/attenuate the noise to ensure quality control of the RFs, so-called Gauss factor. Therefore, the estimated deconvolution was multiplied by the Gaussian pulse to limit the frequency bands and exclude high frequencies not belonging to the original data, generated after deconvolution (Langston, 1979). In this work, the proposal does not include details about the crustal stratification, consequently, the high frequencies of the RFs were suppressed using a Gauss factor equal to 1.5, frequencies up to 1.2 Hz are generally used to estimate crustal thickness (Ligorria and Ammon, 1999). A

maximum number of iterations of 400 and a minimum error of 0.001 were established as RF calculation parameters (Richter, 2014).

Subsequently, a visual selection of the Radial RFs was performed (Zhu & Kanamori, 2000) targeting a better signal-to-noise ratio. Other criteria were also taken into account, the recording of the P wave must be well defined and centered around 0 seconds. As well as, the Ps phase should be registered around 5 seconds after the P. In addition to the other later phases, the multiples are usually registered around 12 to 15 seconds.

3.1.2. *H-k stacking*

Stacking the resulting RFs traces provides greater precision, as it reduces random environmental noise, and as the signal generated in subsurface structures must repeat coherently. Therefore, the amplitudes of these traces are added with the aim of increasing the signal-to-noise ratio.

RFs analysis by station was performed using the *H-k stacking* program, where H is the Moho depth in km and k is the Vp/Vs ratio. An average crustal P-wave velocity (VMVP) value of 6.4 km/s was adopted, based on previous studies (Mooney et al., 1998; Rivadeneyra-Vera et al., 2019; Vera, 2021). To estimate the variation of Moho depth and Vp/Vs ratio as a function of VMVP, H and k were estimated by varying the VMVP between 6.2 and 6.8 km/s. Other input parameters, such as the weights assigned to each of the phases, were also established, the following values were used: Ps equal to 0.6 for the converted phase with the largest amplitude, PpPs (1st multiple) equal to 0.3 and PpPs+PpSs (2nd multiple) equal to 0.1, the sum of these weights is equals 1 (Zhu & Kanamori, 2000). The default maximum and minimum values already provided in the program were used to calculate H and k, which were 20 and 50 km and 1.6 and 1.9, respectively. Finally, the crustal estimates studied here are provided based on these parameters.

3.2. Gravimetric

3.2.1. 3D Gravimetric Inversion

The Bouguer anomaly data used in this study were obtained from the World Gravity Map 2012 (WGM2012) compilation (Bonvalot et al., 2012), with a spatial resolution of 2 minutes. The inversion of the gravimetric data was performed using a program written in MATLAB language, 3DINVER.M (Gómez-Ortiz and Agarwal, 2005), which is based on Parker-Oldenburg's algorithm (Parker, 1973; Oldenburg, 1974).

To estimate the depth of the Moho and its effect on Δg , a 3D inversion was performed using the Δg data. The parameters considered in this calculation were: a smaller cut-off frequency (WH) of 0.01 (1/wavelength in km), a larger cut-off frequency (SH) of 0.015 (1/wavelength in km), a convergence criterion of 0.02, and a truncation of the data window size of 0.1 (10%). The default value of Moho density contrast of 0.7 g/cm³ (taken from CRUST1.0) and a reference depth of 37 km (based on seismological stations) obtained using the average P-wave velocity in the crust (6.4 km/s) were used.

4. Results and discussion

For the PLTB station, in the RF selection step, from the resulting R component, 131 of 402 seismic events

Investigation of Moho depth and crustal composition in the Sul-Rio-Grandense Shield

remained. The trace of each RF (Fig. 3) is plotted in Fig. 3A, as well as the back-azimuth in Fig. 3B, given in degrees.

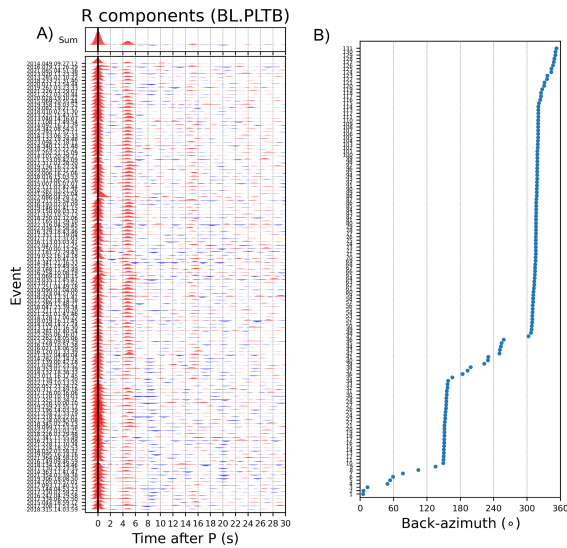


Figure 3 -Receiver Functions selected for the PLTB station. (A) The Radial component. (B) The back-azimuth in degrees.

As seen in Fig. 3B, the station has the highest azimuthal coverage of events at 150° and between 300° and 360° . This result suggests a preferential direction for the arrival of events at the station, indicating the presence of anisotropy and lateral heterogeneities in the middle below the station. The litho-structural heterogeneity of the crust below the station may be a consequence of a large structural complexity, which can be explained by the existing shear zone, nearby sutures (doubling of lower crust) or even by some influence from the Paraná Basin. A total of 131 RF were stacked for this station. The results obtained from the *H-k stacking* inversion (Fig. 4) demonstrate the stacking energy of different phases, namely the converted wave Ps (Fig. 4A), the multiple PpPs (Fig. 4B), the multiple PsPs+PpSs (Fig. 4C), and the final result of $H = 37.0$ and $k = 1.78$ (Fig. 4D).

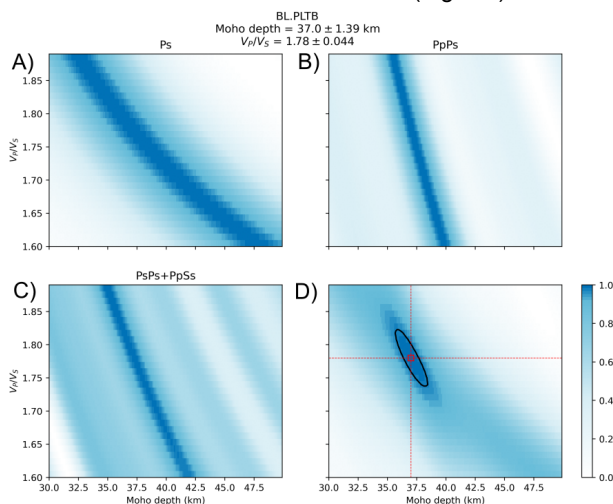


Figure 4 - *H-k stacking* of PLTB station using P wave speed of 6.4 km/s. (A) The converted Ps wave. (B) The

multiple PpPs. (C) The multiple PsPs+PpSs. (D) result of the estimation.

At the CPSB station (Fig. 5), 146 of 409 seismic events were selected in the RF selection step. The results generated with the *H-k stacking* inversion (Fig. 6) show the stacking energy of the different phases, including the converted Ps wave (Fig. 6A), the multiple PpPs (Fig. 6B), and the multiple PsPs+PpSs (Fig. 6C), as well as the final result of $H = 37.2$ and $k = 1.78$ (Fig. 6D).

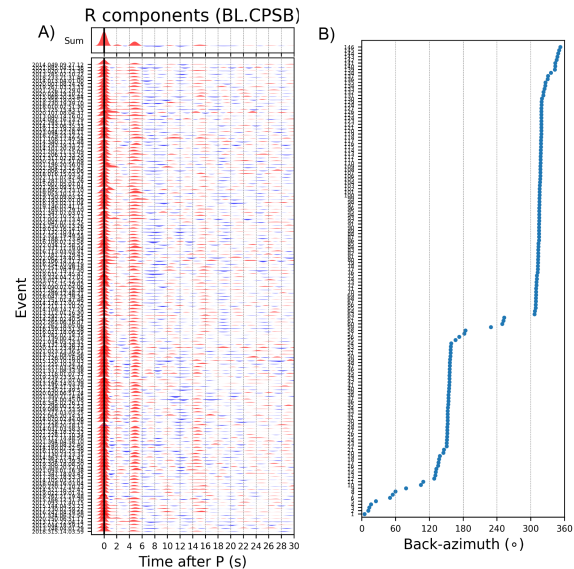


Figure 5 - Receiver functions selected for the CPSB station. (A) The Radial component. (B) The back-azimuth in degrees.

As depicted in Fig. 5B, the largest azimuthal coverage of events is observed between 120° and 170° and between 300 and 360° , indicating an anisotropy and lateral heterogeneities in the medium beneath the station that is similar to PLTB station.

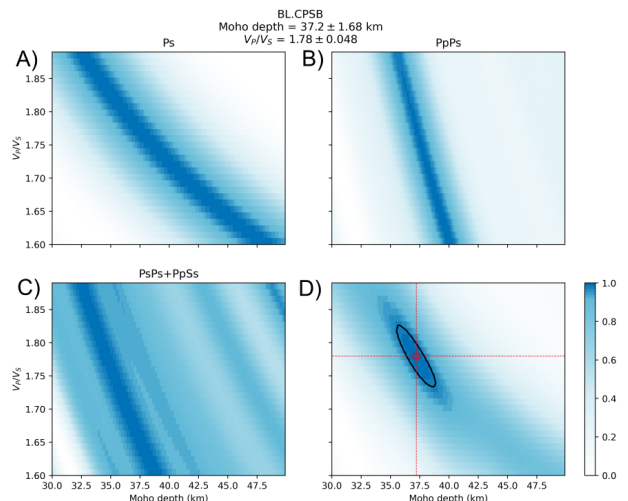


Figure 6 - *H-k stacking* for station CPSB using P wave speed of 6.4 km/s. (A) The converted Ps wave. (B) The multiple PpPs. (C) The multiple PsPs+PpSs. (D) Result of this estimation.

Herzog, I; Coelho, D. L. O; Hispagnol, N. R; Lima, M. V. A. G; Gregory, T. R

The crustal thickness values obtained using different P-wave velocities for each station are presented in Table 2 along with the results obtained from the 3D gravimetric inversion.

The V_p/V_s ratio for the studied is shown in Figures 4 and 6, which is a dimensionless parameter that can provide information about the silica content of the crust, allowing us to infer its composition as mafic, felsic or intermediate (Zandt & Ammon, 1995; Mussachio et al., 1997). Based on the values listed in Table 2, it is possible to infer that the Sul-rio-grandense Shield has a predominantly mafic crust.

		CPSB	PLTB
V_p/V_s	$V_p = 6.2 \text{ km/s}$	1.79 ± 0.049	1.79 ± 0.045
	$V_p = 6.3 \text{ km/s}$	1.78 ± 0.048	1.78 ± 0.046
	$V_p = 6.4 \text{ km/s}$	1.78 ± 0.048	1.78 ± 0.044
	$V_p = 6.5 \text{ km/s}$	1.77 ± 0.047	1.78 ± 0.044
	$V_p = 6.6 \text{ km/s}$	1.77 ± 0.047	1.77 ± 0.043
	$V_p = 6.7 \text{ km/s}$	1.76 ± 0.047	1.77 ± 0.043
	$V_p = 6.8 \text{ km/s}$	1.76 ± 0.046	1.76 ± 0.043

Table 7 - Presentation of the values of the ratio crustal composition parameter (V_p/V_s).

The map of the Bouguer anomaly (ΔBg) (Fig. 7) shows values ranging from 114.51 to 229.05 mGal. Superimposed on the map, the three main tectonic compartments of the SrgS were indicated (Fernandes et al., 1995).

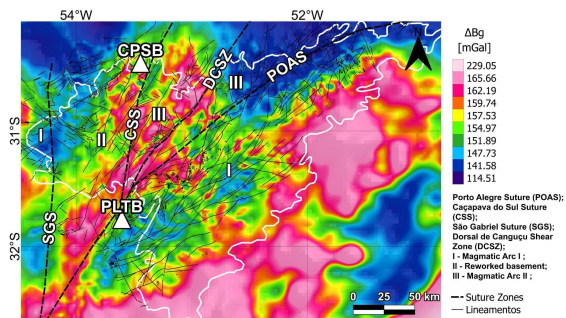


Figure 7 - ΔBg map of the SrgS with the limits of the SrgS (white polygon), the main suture zones (dashed black line), the main lineaments (thin black line) and the seismic stations used (white triangle). The tectonic domains are according to Fernandes et al. (1995).

The Dorsal de Canguçu Shear Zone (DCSZ) in the central tectonic compartment of domain III, which is associated with the reworked basement, is characterized by high values. In contrast, domain I (associated with magmatic arc 1) shows low values, while domain II (associated with magmatic arc 2) exhibits medium to high values, with the high values possibly related to the Caçapava do Sul Suture (CSS).

The map of the estimated depth of the Moho (Fig. 8) shows values ranging from 36.75 and 37.4 km.

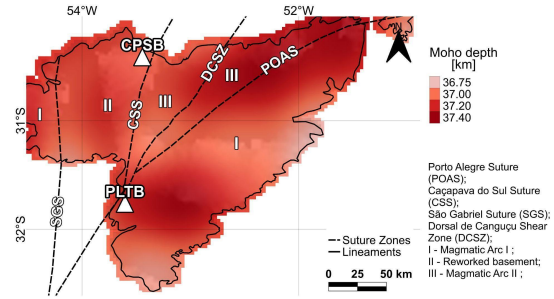


Figure. 8 - Map of the estimated depth of the SrgS Moho with the limits of the SrgS (white polygon), the main suture zones (dashed black line), the seismic stations used (white triangles). The tectonic domains are according to Fernandes et al. (1995).

		CPSB	PLTB
Moho depth [km]	$V_p = 6.2 \text{ km/s}$	$35.7 \pm 1.62 \text{ km}$	$35.6 \pm 1.35 \text{ km}$
	$V_p = 6.3 \text{ km/s}$	$36.6 \pm 1.66 \text{ km}$	$36.4 \pm 1.35 \text{ km}$
	$V_p = 6.4 \text{ km/s}$	$37.2 \pm 1.68 \text{ km}$	$37.0 \pm 1.39 \text{ km}$
	$V_p = 6.5 \text{ km/s}$	$38.1 \pm 1.71 \text{ km}$	$37.6 \pm 1.40 \text{ km}$
	$V_p = 6.6 \text{ km/s}$	$38.6 \pm 1.73 \text{ km}$	$38.5 \pm 1.42 \text{ km}$
	$V_p = 6.7 \text{ km/s}$	$39.5 \pm 1.73 \text{ km}$	$39.1 \pm 1.45 \text{ km}$
	$V_p = 6.8 \text{ km/s}$	$40.1 \pm 1.78 \text{ km}$	$40.0 \pm 1.47 \text{ km}$
Moho_inv depth [km]	37.05	37.18	

Table 2 - Presentation and comparison of Moho depth values obtained by stations and inversion.

Table 2 compares the Moho depth values obtained at each station using the Receiver Function method with different P-wave velocities and the values obtained by the 3D gravimetric inversion (with a P wave velocity of 6.4 km/s) (Moho_inv).

The results obtained using the mean velocity of the P-wave in the crust (6.4 km/s) for both stations are consistent with previous studies (Assumpção et al., 2013; Cruz, 2021; Lima, 2016). The average crustal thickness estimated using the Receiver Function method at the CPSB and PLTB stations were 37.97 km and 37.7 km, respectively. These values are within the expected range for this region, which is located on the boundary of the Shield with the Paraná Basin, and the expected crustal thickness for this region is around 38 km.

The V_p/V_s ratio obtained for each station had an average value of 1.77 (CPSB) and 1.78 (PLTB), which is consistent with the expected range of 1.71 to 1.77 based on previous studies (Rivadeneira-Vera et al., 2019). Therefore, estimates are not associated with the thick basalt layer region located in the Paraná Basin, as the crust in this region is thicker (Rivadeneira-Vera et al., 2019). Consequently, it can be inferred that the depth of

the Moho in the SrgS is more superficial, which suggests the uplift process of this discontinuity, and also highlights the presence of the Rio Grande Arch. The values obtained from the gravimetric inversion are consistent with the average obtained from the Receiver Function method.

5. Conclusions

The integration of seismology and gravimetry methods showed a strong correlation, as observed by the Moho depth results obtained through 3D inversion of the gravimetric data.

Using the Receiver Function (RF) technique, the Moho depth in the regions on the edges of the Sul-rio-grandense Shield (SrgS) was estimated to be approximately 37 km, assuming a mean P wave velocity in the crust of 6.4 km/s.

The gravimetric inversion of Moho revealed values that did not present significant variations, as expected in a crystalline shield. The Moho depth map in Figure 8 shows two regions with values of around 37.3 km.

Based on the Vp/Vs ratio values obtained by RF and previous studies by Zandt & Ammon (1995) and Mussachio et al. (1997), it was concluded that the crust under the stations located in the SrgS is composed of mafic rocks, which is consistent with the geological context of the region.

The crustal thickness and composition results obtained with the average P wave velocity in the crust are consistent with previous works, such as Assumpção et al. (2013), Lima (2016), and Rivadeneyra-Vera et al. (2019).

Acknowledgments

Herzog, I. would like to thank the Internal Program for Scientific and Technological Initiation of the National Observatory (PICT/ON) for granting the Scientific Initiation Scholarship (public notice N°02-2022).

References

ASSUMPÇÃO, M. et al. Crustal thickness map of Brazil: Data compilation and main features. *Journal of South American Earth Sciences*, Elsevier, v. 43, p. 74–85, 2013.

BALMINO, G. et al. 2011. Spherical harmonic modelling to ultra-high degree of Bouguer and isostatic anomalies.

BASEI, M.A.S. 1985. O Cinturão Dom Feliciano em Santa Catarina. São Paulo. 190 p. (Tese de Doutorado, IG-USP).

BONVALOT, S. et al. 2012. World Gravity Map. Commission for the Geological Map of the World. Eds. BGI-CGMW-CNES-IRD, Paris.

BRASIL. Instituto Nacional de Pesquisas Espaciais (INPE). 2008. Topodata: banco de dados geomorfológicos do Brasil. Variáveis geomorfológicas locais. São José dos Campos.

BRITO NEVES B.B. & CORDANI, U.G., 1991. Tectonic evolution of South America during the Late Proterozoic. *Precamb.Res.*, 53: 23-40.

Condori, C. et al. (2017), Crustal structure of north Peru from analysis of teleseismic receiver functions, *Journal of South American Earth Sciences*, 76, 11–24.

Dourado, C.J. et al. (2007). Feições crustais determinadas pela análise azimutal da Função do Receptor, na região da estação sismológica de Rio Claro (RCLB). *Revista Brasileira de Geofísica*, v. 25, 2007.

FERNANDES, L. A. D. et al. (1995)b. Evolução Tectônica do Cinturão Dom Feliciano no Escudo Sul-rio-grandense: Parte II - uma contribuição a partir das assinaturas geofísicas. *Revista Brasileira de Geociências*, 25(4):375-384.

Fischer, K. M. et al. (2010), The lithosphere-asthenosphere boundary, *Annu. Rev. Earth Planet. Sci.*, 38, 551–575, doi:10.1146/annurev-earth-040809-152438.

FOWLER, C.M.R. 1990. The solid earth: an introduction to global geophysics. [S.l.]: Cambridge University Press, p. 472.

FRAGOSO CÉSAR, A.R.S. 1980. O Cráton Rio de la Plata e o Cinturão Dom Feliciano no Escudo Uruguaio-SulRio-grandense. In: CONGR. BRAS. GEOL., 31. Curitiba, 1980. Anais... Curitiba, SBG. v. 5, p. 2879-2892.

FRAGOSO CÉSAR, A.R.S. 1991. Tectônica de Placas no Ciclo Brasileiro: As Orogenias dos Cinturões Dom Feliciano e Ribeira no Rio Grande do Sul. São Paulo. 367 p. (Tese de Doutorado, IG-USP).

FRAGOSO C. et al. 1987. Observações sobre o Cinturão Doa Feliciano no Escudo Uruguaio e correlações coei o Escudo do rio Grande do Sul. III simp. Sul-Bras.Geol.. Atas. 2:791-809. Curitiba.

Kennett, B.L.N. (Compiler and Editor). 1991. "IASPEI 1991 Seismological Tables." Bibliotech, Canberra, Australia, 167 pp.

LIMA, J. N. Aplicação do método de função do receptor para determinação da estrutura da crosta e manto superior sob a região sul do Brasil. Universidade Federal do Pampa, 2016.

Goldstein, P., A. Snoke, (2005), "SAC Availability for the IRIS Community", Incorporated Institutions for Seismology Data Management Center Electronic Newsletter.

GOMEZ-ORTIZ, D. & AGARWAL, B. 2005. 3DINVER.M: A MATLAB program to invert the gravity anomaly over a 3D horizontal density interface by Parker-Oldenburg's algorithm. *Computers & Geosciences - COMPUT GEOSCI.* 31, pp. 513-520. DOI: 10.1016/j.cageo.2004.11.004.

Hamming, R.W. (1974). "Digital Filters". Englewood Cliffs, New Jersey: Prentice-Hall.

HARTMANN, L. A. et al. 2007. Evolução Geotectônica do Rio Grande do Sul no PréCambriano. In: Iannuzzi, R. & Frantz, J.C. (Ed.): 50 ANOS de Geologia: Instituto de Geociências. Contribuições, p. 97-123.

CRUZ, M. et al. Caracterização sismológica da porção Sul da Bacia do Paraná e Escudo Sul-RioGrandense pelo método Função do Receptor, 2021, Sociedade Brasileira de Geofísica (SBGF).

MEGIES, T. et al., ObsPy - What can it do for data centers and observatories?, *Annals of Geophysics* (2011), 54 (1).

MILANI, E.J. 1997. Evolução tectono-estratigráfica da Bacia do Paraná e seu relacionamento com a geodinâmica fanerozóica do Gondwana Sul-ocidental. Tese (Doutorado) —Universidade Federal do Rio Grande do Sul. MILANI, E.J.; FILHO, A.T. 2000. Sedimentary basins of South America.

Tectonic Evolution of South America, InFólio Produção Editorial, Rio de Janeiro, Brasil, v. 31, p. 389–449.

Herzog, I; Coelho, D. L. O; Hispagnol, N. R; Lima, M. V. A. G; Gregory, T. R

- Mooney, W. D. et al., 1998. CRUST 5.1: A global crustal model at 5°x 5°. *J. Geophys. Res.*, 103, 727- 747.
- NARDI, L.V.S. & BITENCOURT, MF. 1989. Geologia, petrologia e geoquímica do Complexo Granítico de Caçapava do Sul, RS. *Revista Brasileira de Geociências*, 153-169.
- OLDENBURG, D.W. 1974. The inversion and interpretation of gravity anomalies. *Geophysics*, 39(4), 776 526–536. doi: 10.1190/1.1440465.
- PARKER, R.L. (1973) The rapid calculation of potential anomalies. *Geophysical Journal of the Royal Astronomical Society*, 31(4), 447–455. doi: 10.1111/j.1365-246X.1973.tb06178.x.
- PRESS, F. et al., *Para entender a Terra* . 4. ed. PortoAlegre: Bookman, 2006. 656 p.
- REMUS M.V.D. 1999. Metalogênese dos depósitos hidrotermais de metais base e Au do Ciclo Brasileiro do Bloco São Gabriel, RS. Tese de Doutorado. Universidade Federal do Rio Grande do Sul- URGs, 170P.
- RIBEIRO, M. 1970. Geologia da Folha de Bom Jardim, Rio Grande do Sul, Brasil. *Bol. Div. Geol. Min. Bras. Rio de Janeiro: DNPM*, v.247, p.1-142.
- RICHTER, T. (2014): Temporal Variations of Crustal Properties in Northern Chile Analyzed with Receiver Functions and Passive Image Interferometry, PhD Thesis, Berlin : Freie Univ., 161 p.
- Rivadeneira-Vera, C. et al., (2019). An updated crustal thickness map of central South America based on receiver function measurements in the region of the Chaco, Pantanal, and Paraná Basins, southwestern Brazil. *Journal of Geophysical Research: Solid Earth*, 124, 8491–8505.
- VERA, J. C. R. New measurements of crustal and lithospheric thickness for the South American platform using the receiver function method, toward a 3D velocity model [doi:10.11606/T.14.2021.tde-15092021-124822]. São Paulo : Instituto de Astronomia, Geofísica e Ciências Atmosféricas, Universidad de São Paulo, 2021. Tesis Doctoral en Geofísica. [citado 2023-05-06].
- VIEIRO E SILVA (VIERO, A. C.; SILVA, D. R. A. (org.). *Geodiversidade do estado do Rio Grande do Sul*. Porto Alegre: CPRM, 2010.
- XU, M. and HE, J., *Seispy: Python Module for Batch Calculation and Postprocessing of Receiver Functions*. *Seismological Research Letters* 2022.
- ZANDT, G.; AMMON, C. J. Continental crust composition constrained by measurements of crustal poisson's ratio. *Nature*, Nature Publishing Group, v.374, n. 6518, p. 152, 1995.
- ZHU, L.; KANAMORI, H. 2000. Moho depth variation in southern California from teleseismic receiver functions. *Journal of Geophysical Research: Solid Earth*, v. 105, n.B2, p. 2969-2980.